EUROPEAN FUSION DEVELOPMENT AGREEMENT

EFDA–JET–PR(00)03

MHD Limiting JET Optimised Shear Performance

T C Hender et al

EFDA–JET–PR(00)03

MHD Limiting JET Optimised Shear Performance

T C Hender, S J Allfrey, B Alper, Y Baranov, D N Borba[1], D Howell, G T A Huysmans[2], O J Kwon[3], M Mantsinen[4].

EURATOM/UKAEA Fusion Association, Culham Science Centre, Abingdon, Oxfordshire, OX14 3DB, UK.
[1]EFDA-JET Close Support Unit, Culham Science Centre, Abingdon, Oxfordshire, OX14 3DB, UK.
[2]Association Euratom-CEA, CEA Cadarache, Saint-Paul-lez-Durance, France.
[3]Taegu University, Taegu, Korea.
[4]Association Euratom-Tekes, Technology Development Centre, Finland.

Preprint of a Paper to be submitted for publication in the Proceedings of the Joint Varenna-Lausanne Workshop

1. INTRODUCTION

In the JET Optimised Shear (OS) regime a combination of Lower Hybrid current drive, Ion Cyclotron Resonance Heating (ICRH) and Neutral Beam Injection (NBI) heating is used during the current rise phase to control the plasma current profile. Typically the high power heating phase is timed such that $q_0 \leq 2.0$, and if a power threshold is exceeded then an Internal Transport Barrier (ITB) forms [1]. This combination of relatively low core magnetic shear and high pressure gradients (at the ITB) represents the conditions in which magnetohydrodynamics (MHD) instabilities such as the infernal mode [2] would be expected to be destabilised.

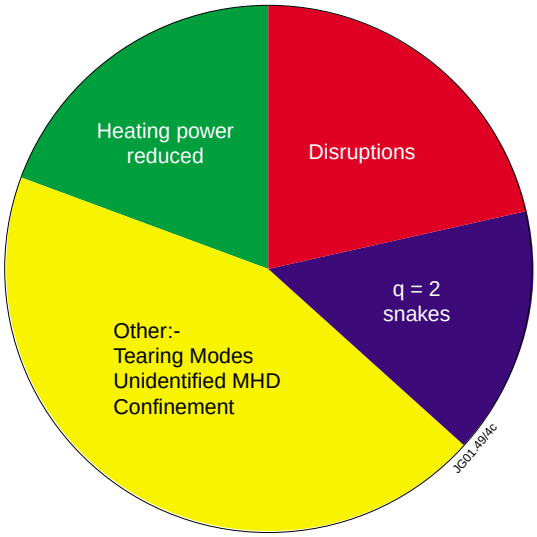

Figure 1: MHD at peak R_{nt} for MKII Gas Box pulses with a neutron yield $R_{nt}>3x10^{16}s^{-1}$. Pulses where the rollover in R_{nt} is due to step-down of heating power, are also identified.

Experimentally the main MHD types observed to limit performance are shown in Figure 1. While disruptions and q=2 snakes are clearly causal in limiting performance, the tearing modes are associated with rather modest reductions in confinement [3]. These 3 main types of performance limiting MHD in OS plasmas and our theoretical understanding of them will be discussed in the remainder of this paper.

2. DISRUPTIONS

There is a good quantitative understanding of disruptions in Optimised Shear plasmas [4] as being due to pressure driven kink modes. In disruptive cases a 'strong' ITB is formed leading to a rapid rise in performance, associated with strong peaking of the pressure (Figure 2).

For the discharge shown in Figure 2 the n=1 stability has been calculated with the MISHKA code [5], based on TRANSP equilibria. The calculated stability limit with no wall, and with a wall at the JET vessel location, are shown in Figure 2 – the normalised β_n at disruption agrees with the calculated limit, with a wall, to within 5%.

This case (pulse 46664) is a discharge in the present MKII Gas Box divertor configuration. Simulations for disruptive OS discharges with the previous MKIIA divertor have shown similarly good correspondence between the calculated β-limit (with the JET wall) for n=1 kink modes and the disruptive limit [4].

Comparisons of the eigenmode structure measured by Electron Cyclotron Emission (ECE) and Soft X-Ray (SXR), with the MISHKA calculations, also shows excellent quantitative agreement.

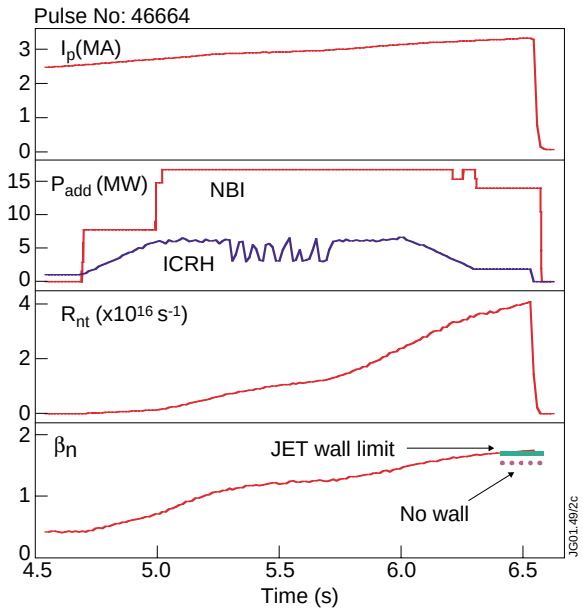

Figure 2: Disruptive OS pulse. The rapid rise in neutron yield (R_{nt}) is associated with strong central peaking of the pressure which drive an n=1 kink mode. The calculated β_n-limits, with and without a wall, are shown.

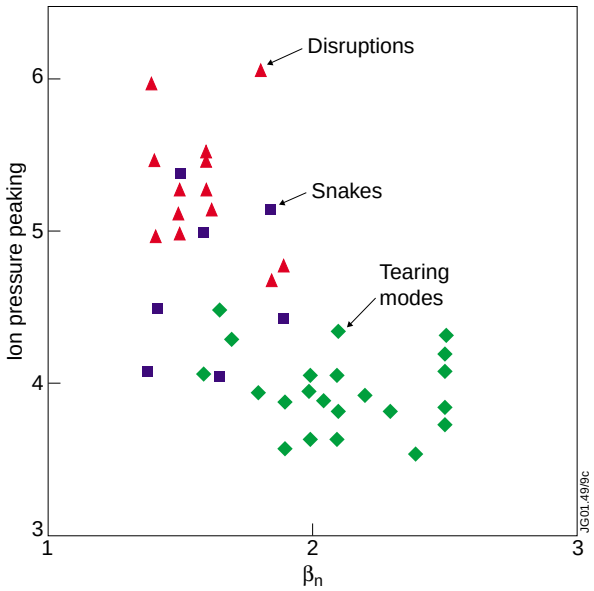

Figure 3: Type of MHD at R_{nt}(max) as a function of pressure peaking and β_n. It can be seen that disruptions occur for the most peaked pressure profiles, snakes for intermediate peaking and tearing modes for the lowest peaking.

While the calculations above show that influence of the wall is a likely explanation for the ability to exceed the no wall stability limit, an alternate explanation comes from the influence of fast particles [6]. OS discharges in JET are low density (typically $n_e(0)<4x10^{19}m^{-3}$) and so the ICRH and beam heating can drive a substantial fast particle population. Moderate frequency (~30–40kHz) chirping modes are often observed and calculations show a likely explanation for them is as a q=2 analogue of fishbone modes [4], driven by resonance with trapped fast particles arising from the ICRH.

As with the q=1 fishbone there is also an analogous stabilisation caused by non-resonant interaction of the trapped fast particles with the kink mode [7] (that is the precursor for disruptions in OS). Calculations with the CASTOR-K code show that an increase of up to about 25% in the β-limit for the kink mode can be expected from this effect [6]. Thus fast particle stabilisation provides an alternate explanation for the ability of OS shear discharges to exceed the no-wall β-limit. This explanation is supported by stability calculations for a disruptive NBI-only heated OS discharge, which has a substantially lower fast particle content; in this case n=1 stability calculations show the disruption occurs close to the no-wall stability limit. These OS disruptions are driven by strong peaking of the plasma pressure. By applying the heating at a slightly later time, and in a more progressive fashion, so that the ITB, which approximately tracks the q=2 location, has time to expand, the over-peaking and resulting disruption can be avoided. However, for slightly less peaked discharges a performance limit is set by the q=2 snake (Figure 3). Further reducing the pressure peaking by tailoring the heating and puffing Argon (which cools the edge aiding current penetration and moderating Electron L-Mode (ELMs)), avoids both disruptions and snakes, leaving moderate-n tearing modes as the main residual MHD in these high-β_n discharges. We now go on to examine the snake instability in more detail.

3. q=2 SNAKES

The q=2 snake is a spatially localised feature associated with the q=2 surface. It is visible on edge magnetic probes and the associated perturbations to the plasma are visible on SXR and ECE diagnostics (Figure 4). The snake is causal in limiting performance in OS discharges. The action of the snake is to erode the ITB inwards (Figure 5), which causes an increased outflow of energy and a resultant transition to large ELMs – these large ELMs tend to cause an irreversible loss of the OS regime, though strong puffing of Argon can control the ELMs and then repeated cycles of snakes and degradation of the ITB can result (an example is shown in Figure 9).

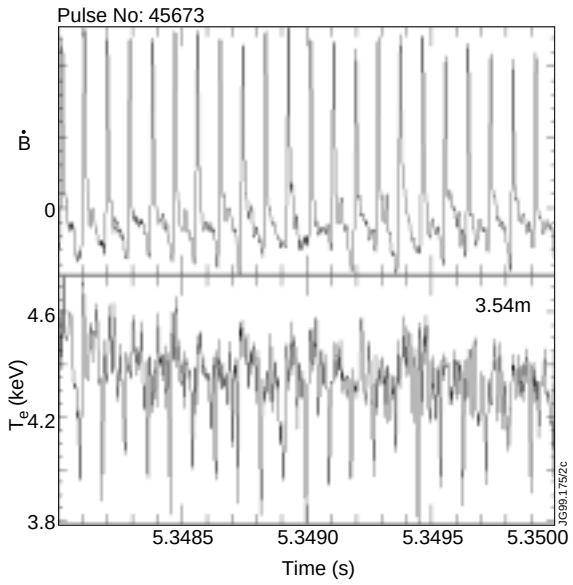

Figure 4: Magnetic and electron temperature perturbations associated with the snake.

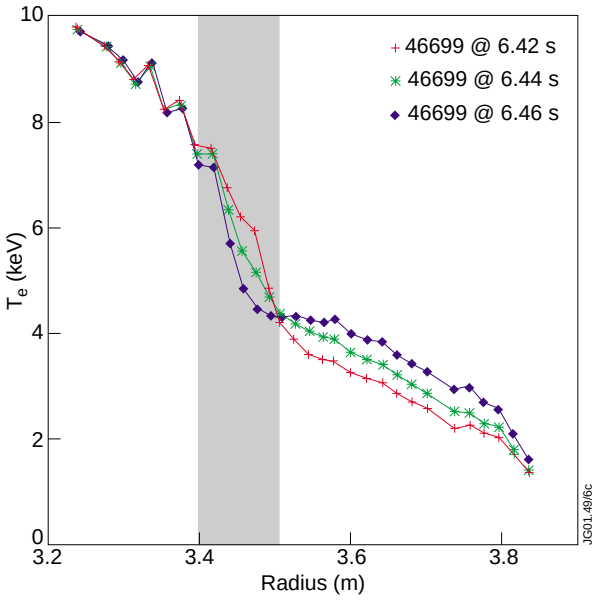

Figure 5: Erosion of temperature profile at ITB resulting from snake.

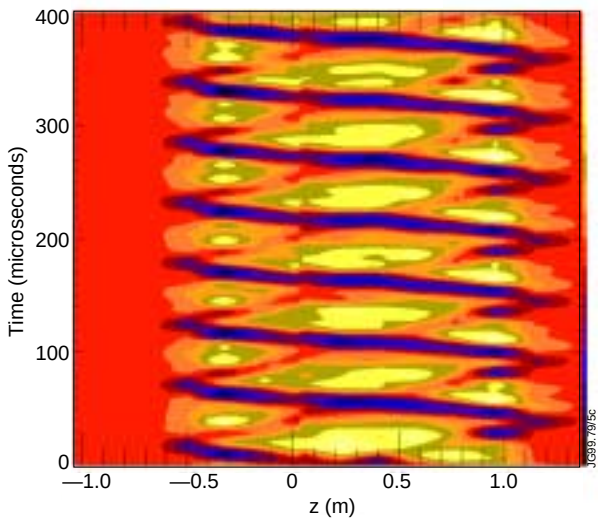

Figure 6: Contours of SXR emission as a function of vertical height of the SXR chord. The time averaged background SXR signal is subtracted. The snake structure consists of 2 interlaced helicies.

The SXR perturbations associated with the snake (Figure 6) show a double helix structure – strongly suggesting a structure localised along a q=2 field line (like conventional snakes are localised to a q=1 field line [8]).

The magnetic perturbations arising from the snake are well modelled by a wire filament which follows a q=2 field line (Figure 7(a)). Matching the amplitude of the measured magnetic signals shows this filament caries only a very small current (<0.04% of the plasma current) as shown in Figure 7(b). Given the radial extent of the snake perturbation, O (10cm), this small current in the snake implies a locally low magnetic shear, $rq'/q \sim 0.2$

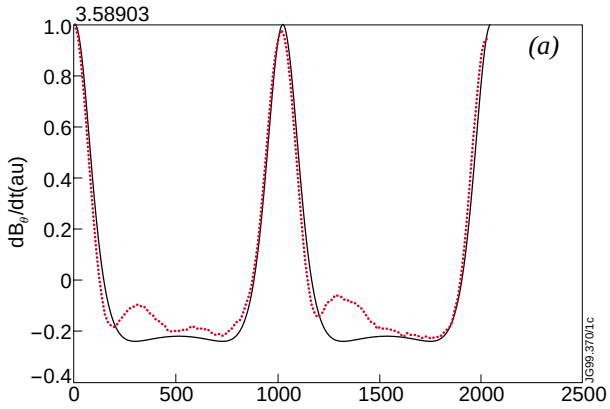

Figure 7(a): Measured db_θ/dt signal from snake (dotted line) and fit resulting from q=2 wire filament model.

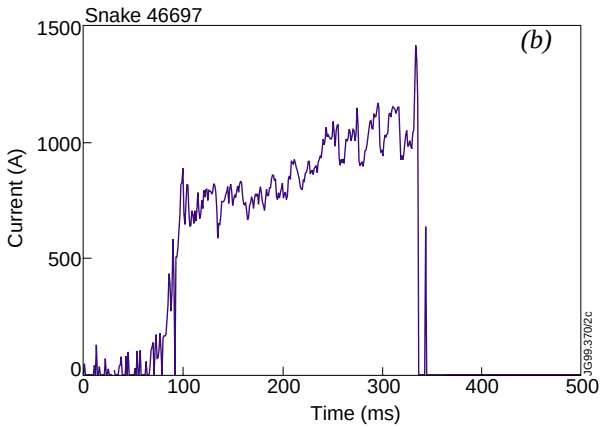

Figure 7(b): Current carried in snake filament (for a plasma with a current of 3.3MA)

The topology of the snake, which shows no change in phase with radius (Figure 8(a)), also hints at the local shape of the q-profile – if the q-profile were locally monotone increasing or decreasing at q=2 then a single wire filament would produce a magnetic island structure. Instead the q must be at a local extrema at q=2, for which a q=2 current filament generates no phase inversion and shows good agreement with ECE observations (Figure 8(b)). The current in the snake filament is measured to be anti-parallel to I_p and to attain the correct magnetic topology requires that q be at a local maxima. A drive mechanism for the current in the snake comes from the local reduction of temperature in the snake, which increases the resistivity, and excludes current from the snake (ie effectively drives current anti-parallel to I_p) [9].

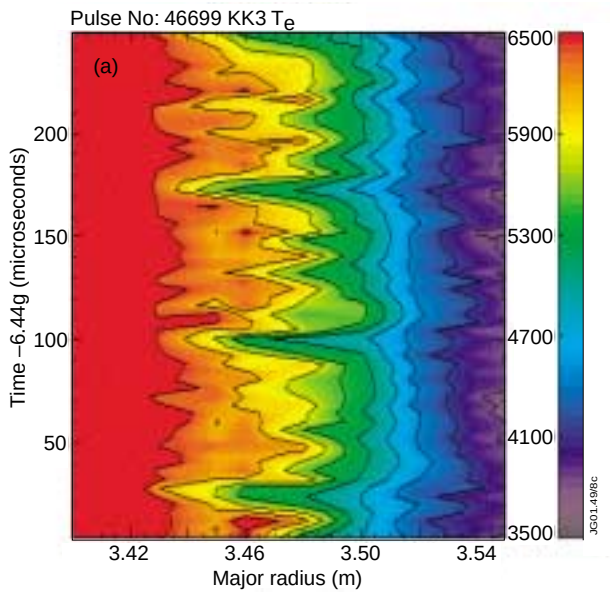

Figure 8(a): Temperature contours for a q=2 snake in pulse 46699 .

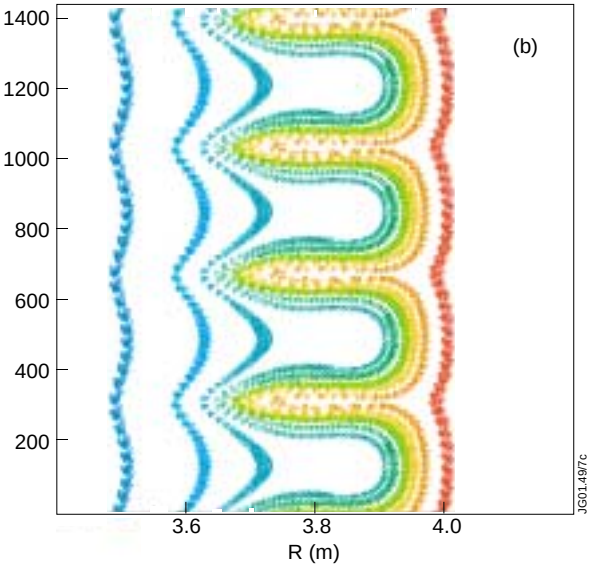

Figure 8(b): Flux surfaces for a current filament on a q=2 field for a q-profile with q_{min}=2 (this figure is intended to show the correct topology attained with a q=2 current filament at an extrema and is not intended as a detailed simulation of the experiment)

A feature of the snake which is consistent with the above model for driving current in the snake is the ability of it to flip from positive to negative variations of the temperature, at a given radius, in a few 100ms. Since both the temperature and magnetic phase flip together it is concluded that the current in the snake reverses its sign. In this case the increased temperature in the snake drives current parallel to I_p and will produce the opposite direction of flux surface distortions, as required. It remains to complete this picture of the snake by explaining how, from an equilibrium and transport viewpoint, a local maximum can occur at q=2. It seems likely that the steep rise in temperature from the foot of the ITB inhibits current penetration causing a local minimum in q and, at a smaller minor radius, a corresponding local maximum. Detailed transport simulations are in progress to test this point.

4. MODERATE-N TEARING MODES

Establishment of broader ITBs, by the delaying of high power heating and Argon puffing, can avoid both disruptions and q=2 snakes (Figure 3). These broader ITBs can access higher β_n, due to the larger volume within the ITB, and in these conditions moderate-n (n~3 to 6) tearing modes are often observed (Figure 9). The ITB regime is not terminated by these moderate-n tearing modes, though there is evidence for modest confinement degradation associated with these modes [3].

In some discharges, including that shown in Figure 9, the tearing modes can co-exist with q=2 snakes. The radial location of the tearing mode is found to be just within the q=2 snake. These tearing modes have the property that the phase between the magnetic island (observed by ECE) and the edge magnetic perturbation can change by 180^o; such a change in phase occurs just before t=6s for the n=6 mode shown in Figure 9. The most plausible explanation for this flip in phase is that the magnetic shear reverses sign at the tearing modes rational surface. This means that the drive for these tearing modes can not be solely the neo-classical term as this is stabilising for (*dq/dr<0*). Also the fact that these modes grow from noise with no obvious seed island (Figure 10) tends to suggest the modes are not solely driven by neo-classical terms.

A source of drive for moderate-n modes, when the magnetic shear is sufficiently negative, comes from the resistive interchange terms and this has been identified as being associated with instabilities observed in DIII-D negative shear discharges [10]. For *dq/dr<0* then the necessary condition for resistive interchange instability, $D_R>0$, can be satisfied even when q~2:

$$D_R = \frac{\beta_0}{r}\left(\frac{q'}{q}\right)^2 \frac{dP}{dr}\left(q^2 - 1 + \frac{q^3 q'}{r^3}\int_0^r \left[\frac{r^3}{q^2} - \frac{r^2}{\varepsilon^2}\beta_0 \frac{dP}{dr}\right]dr\right) \qquad (1)$$

But coupling to stable tearing modes (at large-m Δ'~-2m/r_s) can stabilise the interchange mode and the condition:

$$-\Delta' < \frac{2.74}{\hat{s}^{1/2}}(\hat{s}D_R)^{5/6}\left(\frac{S}{n^2}\right)^{1/3} \quad with \quad \hat{s} = \frac{r\,|\,q'\,|}{q} \qquad (2)$$

must also be satisfied for instability. Calculations of resistive stability have been made using the FAR code [11] for the model q-profiles shown in Figure 11. It is found for sufficient shear that moderate-n modes are destabilised, as shown in Figure 12 for the n=4 (dominantly m=9) mode.

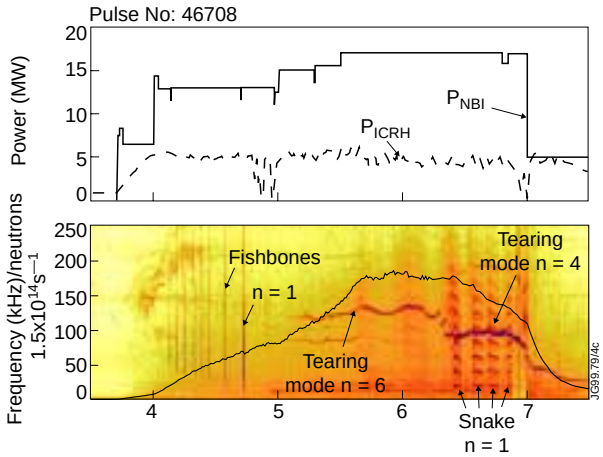

Figure 9: Discharge at high-β_n (~2.5) which exhibits a succession of moderate-n tearing modes. This discharge also has a series of simultaneous q=2 snakes.

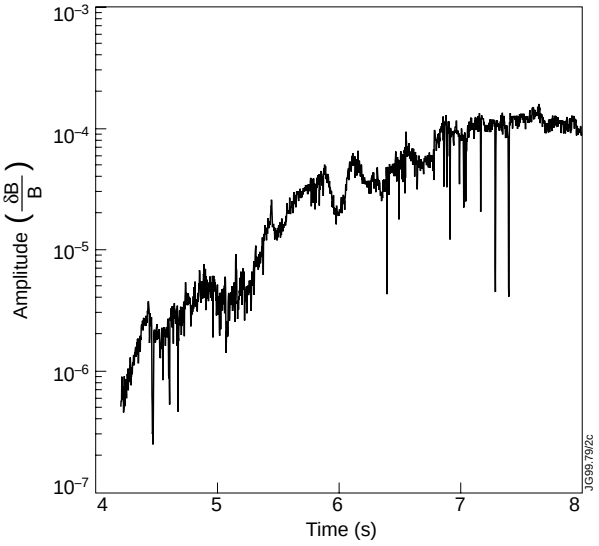

Figure 10: Amplitude of tearing mode showing it grows from a very small size, with no obvious seed.

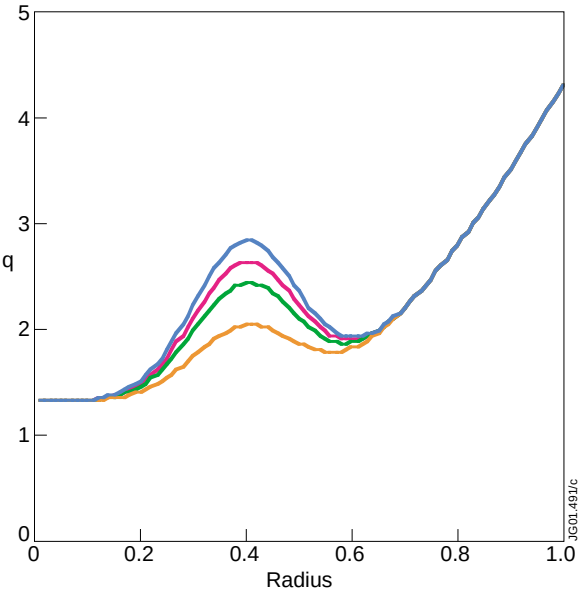

Figure 11: q-profile family used in study of resistive interchange stability

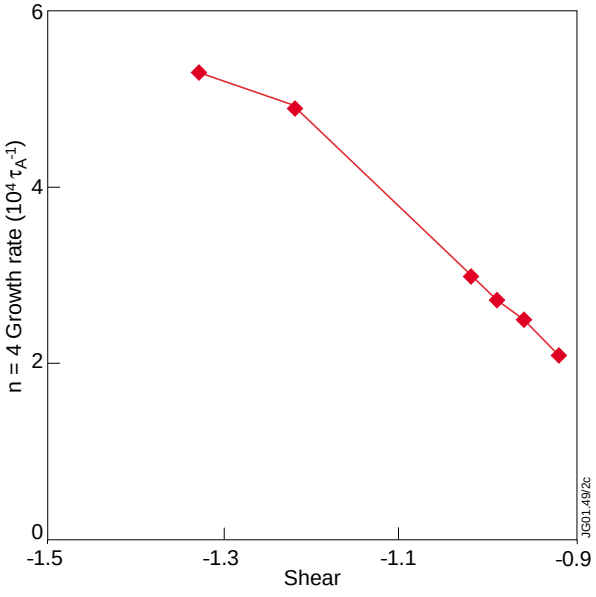

Figure 12: Growth rate for n=4 resistive interchange mode.

A problem is that for typical magnetic Reynolds numbers in JET, S~O(10^8) (near the foot of the ITB), the most unstable toroidal mode number is higher than observed (Figure 13); this increase in unstable-n with S is expected from Eqn (2). Though of course FLR terms may contribute to stabilising the higher-n resistive interchange modes. Also the magnetic islands show a strong radial in-out asymmetry, whereas the observed plasma displacement (from ECE) is quite

symmetric. Thus further studies are clearly required to fully understand the nature of the observed moderate-n tearing modes.

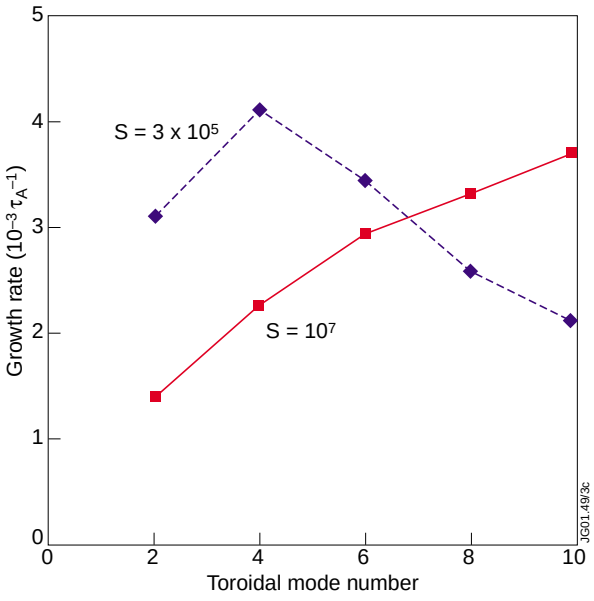

Figure 13: Growth rate of resistive interchange mode as a function of toroidal mode number for an equilibrium with a shear at q=2.25 of -0.88.

5. SUMMARY AND DISCUSSION

MHD instabilities are the main, though not the only, cause of performance limitation in OS discharges. Non-MHD causes can include contact with material surfaces such as the divertor septum [12] and spontaneous transitions to reduced confinement. Of the MHD limits the most fundamental is the n=1 pressure driven kink mode, which leads to a disruption. The β-limit due to this mode can be increased somewhat by wall and fast particle stabilisation, but ultimately a limit is set on the attainable β_n at a given pressure peaking. Optimisation of performance in the OS regime is achieved by closely approaching the disruptive limit and so some method of real-time feedback is desirable, for which the real issue becomes how to detect the approach to instability. One promising approach is to use the internal saddle coils in JET and monitor the response to applied low frequency perturbations (10-50kHz) [13].

The stability of the kink mode is governed by the dispersion relation $\omega(\omega-\omega^*_i)=-\gamma^2_{MHD}$ and as instability is approached 2 damped modes approach each other in frequency. These damped modes can be monitored by the response to the applied saddle fields and the difference in frequency provides a measure of how close instability is from occurring.

After disruptions the next most significant instability is the q=2 snake, whose occurrence generally terminates the ITB. A lot of progress has been made in understanding the physics of these snakes, which extends to important implications on the nature of the q-profile. The least significant instability class, in terms of effects on the ITB, is the moderate-n tearing modes.

The apparent ability of these modes to persist in both positive and negative shear indicates they may be driven (and damped) by both neo-classical and resistive interchange mode terms, but further work is needed on this issue.

So in summary, a lot of progress has been made in understanding the nature of MHD instabilities in JET OS plasmas which is important both from the viewpoint of optimising performance and also for the information it provides on q-profile evolution.

ACKNOWLEDGEMENTS

This work was conducted partly in the framework of the JET Joint Undertaking and partly under the European Fusion Development Agreement. This work was jointly funded by EURATOM and the UK Department of Trade and Industry. The work of Dr Kwon was completed during a visit in 1999, which was supported in part by Taegu University Research Grant 1999.

REFERENCES

[1] C Gormezano et al, Phys Rev Lett **80** (1998) 5544.
[2] J Manickam et al NF 27 (1987) 1460
[3] Y Baranov et al, 1999 26th EPS Maastricht, CD-ROM Vol 23J p169
[4] G T A Huysmans Nucl Fusion **39** (1999) 1489
[5] A B Mikhailovskii et al, Plasma Phys Rep **23** (1997) 844
[6] D N Borba et al, 1999 26th EPS Maastricht, CD-ROM Vol 23J p221
[7] P Helander et al, Phys Plasmas **4** (1997) 2181
[8] R D Gill et al, Nucl Fus **32** (1992) 723
[9] B Alper et al, 1999 26th EPS Maastricht, CD-ROM Vol 23J p173
[9] M S Chu et al, Phys Rev Lett **77** (1996) 2710.
[10] L A Charlton et al, Jrnl Comp Phys **86** (1990) 270
[11] C Gormezano et al, 2000 27th EPS Budapest, paper P1.048.
[12] D Testa et al, 2000 27th EPS Budapest, paper P4.044.